

Erasable superconductivity in topological insulator Bi_2Se_3 induced by voltage pulse

Tian Le ^{*1,2}, Qikai Ye³, Chufan Chen², Lichang Yin², Dongting Zhang², Xiaozhi Wang
^{†3}, and Xin Lu ^{‡2,4,5}

¹*Beijing National Laboratory for Condensed Matter Physics, Institute of Physics,
Chinese Academy of Sciences, Beijing 100190, China*

²*Center for Correlated Matter and Department of Physics, Zhejiang University,
Hangzhou 310058, China*

³*Key Laboratory of Advanced Micro/Nano Electronic Devices and Smart Systems of
Zhejiang, College of Information Science and Electronic Engineering, Zhejiang
University, Hangzhou 310027, China*

⁴*Zhejiang Province Key Laboratory of Quantum Technology and Device, Zhejiang
University, Hangzhou 310027, China*

⁵*Collaborative Innovation Center of Advanced Microstructures, Nanjing University,
Nanjing, 210093, China*

Three-dimensional topological insulators (TIs) attract much attention due to its topologically protected Dirac surface states. Doping into TIs or their proximity with normal superconductors can promote the realization of topological superconductivity (SC) and Majorana fermions with potential applications in quantum computations. Here, an emergent superconductivity was observed in local mesoscopic point-contacts on the topological insulator Bi_2Se_3 by applying a voltage pulse through the contacts, evidenced by the Andreev reflection peak in the point-contact spectra and a visible resistance drop in the four-probe electrical resistance measurements. More intriguingly, the superconductivity can be erased with thermal cycles by warming up to high temperatures (300 K) and induced again by the voltage pulse at the base temperature (1.9 K), suggesting a significance for designing new types of quantum devices. Nematic behaviour is also observed in the superconducting

*Corresponding author: tianlephy@iphy.ac.cn

†Corresponding author: xw224@zju.edu.cn

‡Corresponding author: xinluphy@zju.edu.cn

state, similar to the case of $\text{Cu}_x\text{Bi}_2\text{Se}_3$ as topological superconductor candidates.

So far, various methods such as doping, proximity effect, hydraulic pressure, tip-contact have been applied on nontrivial topological materials in order to induce topological superconductivity and Majorana fermions [1, 2, 3, 4, 5, 6, 7]. Majorana fermions are proposed to play a crucial role in the fault-tolerant quantum computation [8, 9, 10]. Among them, Bi_2Se_3 has served as a characteristic compound of topological insulators susceptible to tuning and emergence of superconductivity [1, 2, 5] and its van der Waals (vdW) structure also implies a potential application in quantum electronic devices, especially when superconductivity can be achieved [11, 12, 13]. However, an easy and controllable condition to realize SC in Bi_2Se_3 is still lacking and thus desirable.

In this paper, an unambiguous superconductivity is observed for the mesoscopic point-contacts on topological insulator Bi_2Se_3 after applying a voltage pulse, evidenced by the Andreev reflection peak in point-contact spectra (PCS) and a resistance drop for the exfoliated Bi_2Se_3 flake samples. Superconductivity emerges only in the case of Ag- Bi_2Se_3 contacts with either silver paints in soft-PCS (SPCS) or Ag tips in mechanical-PCS (MPCS) right after the voltage pulse, but is absent for the Au, Cu or Ti tips, favoring the scenario that the emergent SC is probably due to Ag dopants into the vdW gap of Bi_2Se_3 across the interface. The SC becomes unstable against thermal cycles and disappears when the sample is warmed up to high temperatures, however, it can be re-induced by a new voltage pulse after cooled back to 1.9 K. Our observations strongly support the erasable nature of the SC in the local contact region, ensuring potential applications in quantum devices.

The Bi_2Se_3 crystal is composed of alternating Se-Bi-Se-Bi-Se quintuple layers as shown in Fig. 1a and there exists a weak vdW gap between adjacent quintuple layers, making this material easy to be exfoliated as other vdW materials. Temperature dependent resistivity of Bi_2Se_3 with a sample size of $1073 \mu\text{m} \times 591 \mu\text{m} \times 6.3 \mu\text{m}$ is shown in Fig. 1b, which has a slight upturn due to its insulating band gap but saturates below 40 K with its gapless surface state, consistent with previous reports [14, 15]. Soft point-contacts are formed by silver paints on Bi_2Se_3 as in Fig. 1c, same as the soft-PCS configuration on $\text{Cu}_x\text{Bi}_2\text{Se}_3$ [16]. Fig. 1d shows the soft-PCS conductance curve on Bi_2Se_3 at 1.9 K and only an asymmetric background is observed in the absence of any special features. Interestingly, when a voltage pulse between 4 -10 V with a pulse duration less than 10 ms is applied across the contacts, a reproducible zero-bias conductance peak (ZBCP) can be observed with dips at high bias voltages as in Fig. 1e. Fig. 1f shows the evolution of conductance curves in magnetic field and the ZBCP is gradually suppressed without any peak splitting and finally disappears around 3.0 T. Moreover, the ZBCP gets weaker in intensity with increased temperatures until around 4.5 K, unambiguously signaling the Andreev reflections and induced superconductivity in the contact area by voltage pulses [17, 6, 7]. The maximum

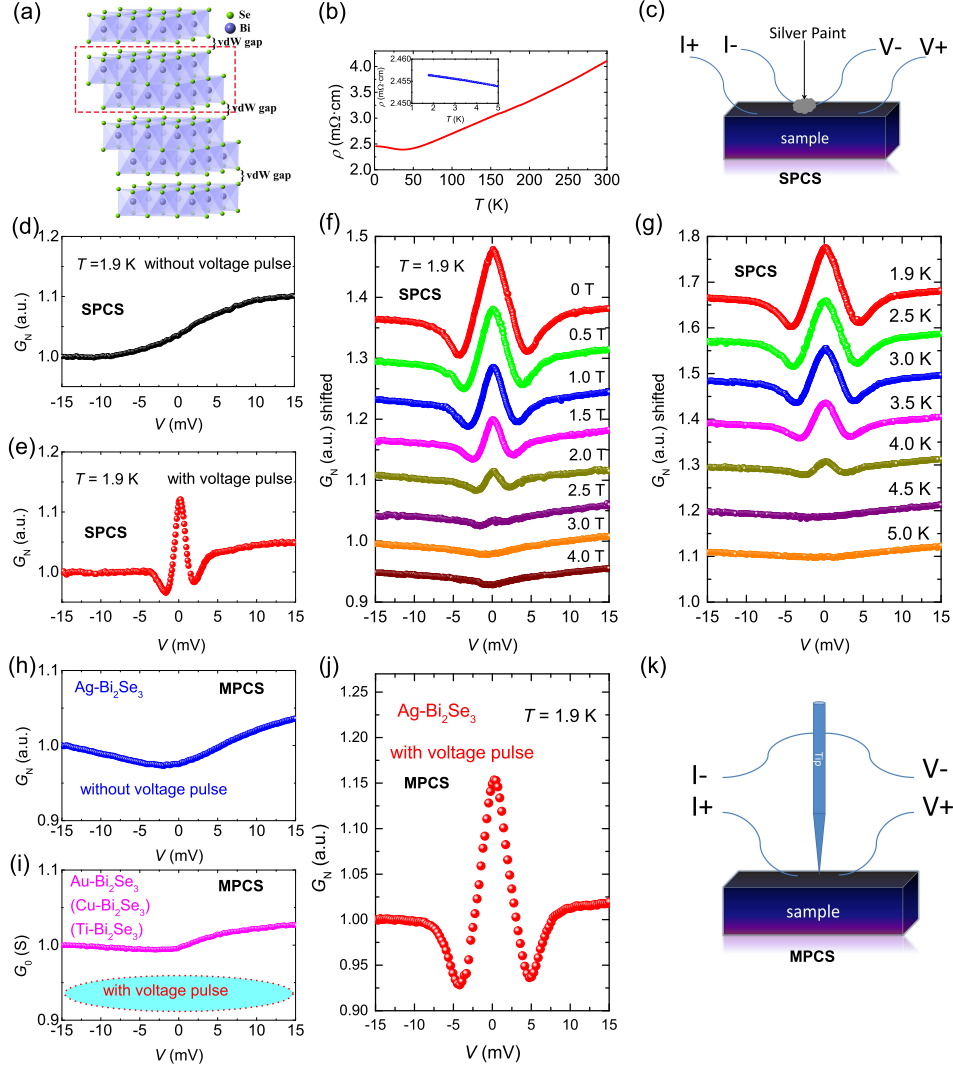


Figure 1: **Evidence for induced superconductivity in mesoscopic Ag point-contact on Bi_2Se_3 .** (a) The crystal structure of topological insulator Bi_2Se_3 with vdW gap between adjacent Se-Bi-Se-Bi-Se quintuple layers. (b) Temperature dependence of the electrical resistivity for the pristine Bi_2Se_3 sample with a dimension of $1073 \mu\text{m} \times 591 \mu\text{m} \times 6.3 \mu\text{m}$. (c) Schematic illustration of the soft-PCS electrode configuration on Bi_2Se_3 . (d) A representative soft-PCS conductance curve for silver paint on the Bi_2Se_3 crystal at 1.9 K without any voltage pulse. G_N is the normalized conductance divided by the conductance value at high voltages. (e) A reproducible ZBCP feature in the soft-PCS at 1.9 K after voltage pulse on the contact. (f) & (g) Magnetic field and temperature evolution of the soft-PCS conductance curves with induced superconductivity in the contact region, respectively. (h) & (i) Mechanical-PCS conductance curve at 1.9 K for Ag tip before voltage pulse and for Au, Cu or Ti tip after voltage pulse, respectively. (j) Mechanical-PCS conductance curve at 1.9 K for Ag tip with induced SC after voltage pulse. (k) Schematic illustration of the needle-anvil configuration of mechanical point-contacts.

superconducting transition temperature T_c for all contacts can be as high as 4.5 K as illustrated by the temperature dependent conductance curves on Bi_2Se_3 in Fig. 1g (or the temperature dependent zero-bias conductance (ZBC) in Fig. S1). We note here that the ZBCP only appears on the contact affected by the voltage pulse and other contacts without it on the same sample would not show any SC trace (Several soft point-contacts on the same sample can be realized in practice). The width of the ZBCP not only depends on the intensity of voltage pulse, but also influenced by detailed contact conditions, such as contact area and contact resistance, and more details can be referred in Supporting Information.

In comparison with our soft-PCS results, a needle-anvil type of mechanical-PCS was also applied as schematically illustrated in Fig. 1k with several tip options available such as silver, gold, copper or titanium. Similar behaviours are observed for the Ag tip on Bi_2Se_3 crystals after a voltage pulse, where a local SC in the contact can be induced with a characteristic SC ZBCP at 1.9 K. In sharp contrast, Au, Cu or Ti tips on Bi_2Se_3 fail to induce any SC within the maximum voltage pulse ~ 10 V as in Fig. 1i. We would thus speculate that the induced SC in the point-contact area is intimately associated with Ag atoms as a result of voltage pulses.

In order to confirm the probable superconductivity with electrical resistive measurements, the Bi_2Se_3 sample was exfoliated by tape to a very tiny flake and it was transferred onto the pre-deposited Ag electrodes on the silicon substrate as shown in the inset of Fig. 2a, where the space between the neighboring electrode ends is about $3 \mu\text{m}$ in distance. The temperature dependent electrical resistance for the pristine device is shown in Fig. 2a, which also has an upturn at low temperatures as in Fig. 1b for the bulk sample. Once voltage pulse is applied on the Ag electrodes, a small drop of resistance shows up below 4.5 K ($\sim 1 - 2\%$) as in Fig. 2a, implying an induced SC as in the PCS measurements. However, the resistance does not go to zero and it is natural to assume a local SC is induced only in the contact region for the Bi_2Se_3 sample. In Fig. 2b, the T_c decreases with increased magnetic field, and the SC transition is totally gone above 2.5 T.

It is interesting to study the stability of this local superconductivity against thermal cycles and the sample resistance over several thermal cycles with a cooling (warming) speed of 3 K/min is shown in Fig. 2c. For the first cycle, the sample is only warmed up to 50 K and then cooled back to 1.9 K, where the SC transition temperature T_c nearly maintains the same value of 4.5 K with the resistance curves overlapping on each other. However, as long as the sample is warmed up to a higher terminal temperature, T_c is gradually reduced and the transition finally disappears after warming up to 300 K. Moreover, superconductivity would emerge once again at 1.9 K after a new voltage pulse on Bi_2Se_3 . Meanwhile, our soft-PCS with silver paint shows a consistent behaviour: the ZBCP would disappear in the conductance curves while the zero-bias conductance as a function of temperature shows the absence of any SC transition after thermal

cycles as in Fig. 2d. It is thus a strong evidence for the metastable nature of induced SC in the mesoscopic Ag point-contacts on Bi₂Se₃, which can be repetitively erased by thermal activations.

As for the underlying mechanism of the induced superconductivity in the Ag-Bi₂Se₃ type point-contacts, the voltage pulse can usually generate a considerable local electric field and inject the metallic atoms from the tip to Bi₂Se₃ [18]. As shown in Fig. 2e, the injected Ag atoms should probably be trapped by and intercalated into the vdW gap of Bi₂Se₃ at low temperatures, forming some kind of Ag_xBi₂Se₃ with superconductivity in the local region similar to the SC compound Cu_xBi₂Se₃. We notice that SC in Ag_xBi₂Se₃ has been theoretically proposed via the dynamic mean-field theory with a local density approximation and its T_c is estimated around 4.5 K, pretty similar to our experimental results [19]. It is actually a common practice for atoms to be deposited on substrates in scanning probe microscopic lithography with the help of a voltage pulse on metallic tip [20, 21, 22]. In general, the atomic emission process is strongly dependent on the evaporation field for different atoms, where Ag has a relatively lower evaporation field in comparison with Cu and Au [18, 23, 24]. On the other hand, even though Ti has a much lower evaporation field than Ag, the intercalation of Ti in Bi₂Se₃ probably would not induce SC as in Ag_xBi₂Se₃ [19]. Of course, the real atomic emission process can be more complicated and more detailed studies are further needed [18, 25].

The disappearance of superconductivity in the Ag-Bi₂Se₃ mesoscopic point-contacts over thermal cycles probably originates from the instability of Ag intercalation in the Bi₂Se₃ vdW gaps at high temperatures. Considering the weak vdW gap between the Bi₂Se₃ quintuple layers, it is not surprising that no Ag_xBi₂Se₃ compound has been reported to be synthesized at room temperatures so far. At 300 K, the intercalated Ag atoms would have escaped from the vdW gap thanks to the thermal activation energy. In comparison, even though SC in Cu_xBi₂Se₃ crystals has been widely reported, its superconducting volume fraction shows a high dependence on quench conditions, where quenching from a lower temperature or not quenching at all can be detrimental to SC, strongly supporting the metastable nature of Cu intercalation [26]. A metastable superconductivity by thermal cycles has also been reported in IrTe₂ with charge-density-wave (CDW) order as its ground state. For IrTe₂, a thermal quench process achieved by current pulses can induce or erase the SC in a tiny exfoliated sample, and it is a kinetic and nonequilibrium approach to induce SC as a metastable state competing with the CDW order [27, 28]. In our case of Bi₂Se₃, the voltage pulse on point-contact can locally heat it to high temperatures and then rapidly cool down, mimicking the thermal quench process. However, the absence of SC in Au, Cu and Ti point-contacts on Bi₂Se₃ argues against the same SC mechanism as in IrTe₂, but favors the importance of Ag intercalation (Refer to Supporting Information for more discussions to exclude local strain, structural changes or impurity phase by voltage pulses as the the origin of superconductivity).

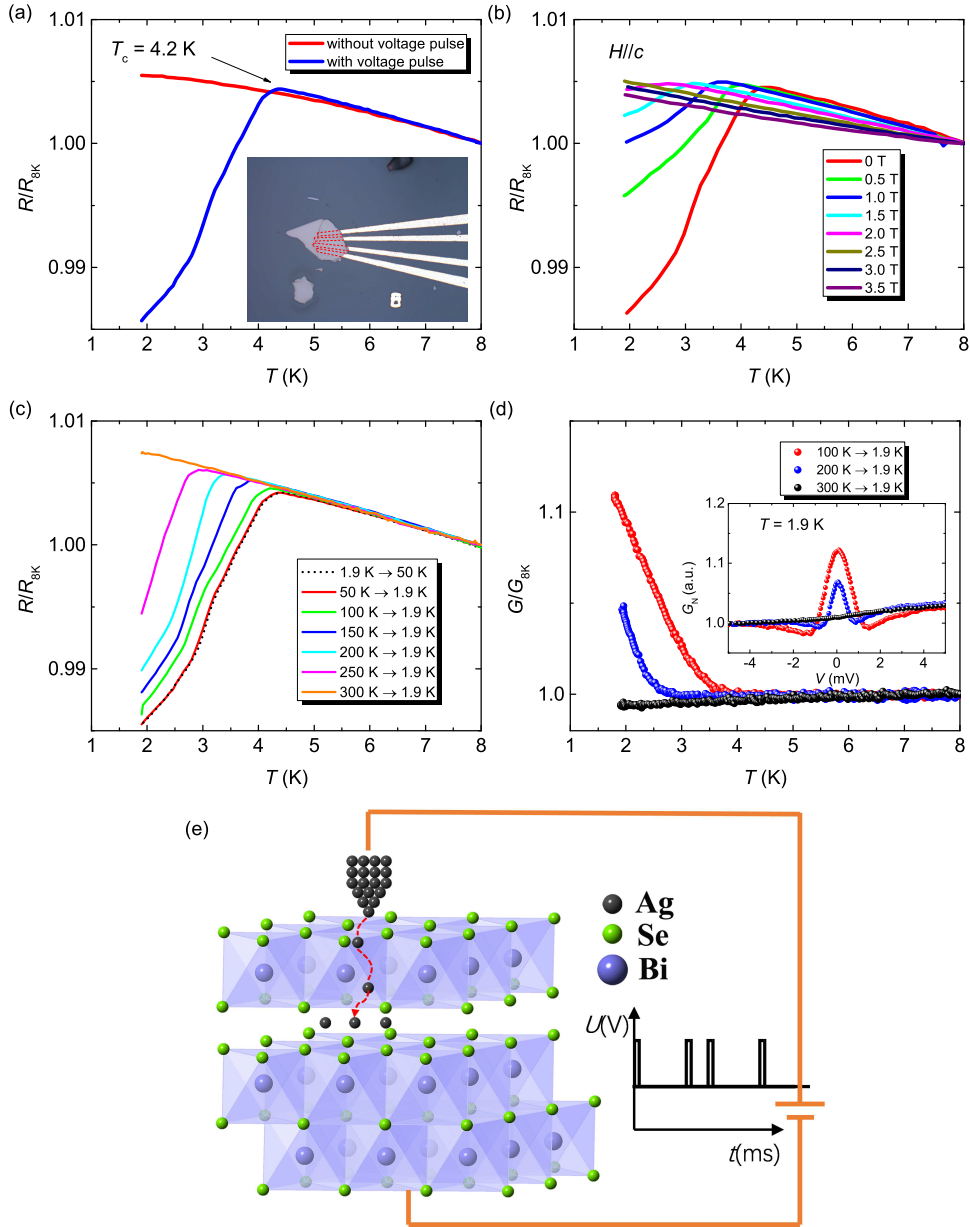


Figure 2: **Evidence of local and erasable superconductivity in Ag-Bi₂Se₃ contacts.**

(a) Temperature dependence of the electrical resistance for an exfoliated Bi₂Se₃ flake before and after voltage pulse for comparison. The inset is the photo of an exfoliated flake with Ag electrodes pre-deposited on the bottom with the electrode distance $\sim 3 \mu\text{m}$. (b) The evolution of R-T curves in different magnetic fields for the exfoliated Bi₂Se₃ sample after voltage pulse. (c) & (d) Temperature dependence of the electrical resistance for exfoliated Bi₂Se₃, and ZBC for silver paint point-contacts after different thermal cycles with a temperature ramping speed of 3 K/min. The inset of (d) shows the Ag-Bi₂Se₃ point-contact conductance at 1.9 K after different thermal cycles. (e) Schematic illustration of Ag atoms locally trapped in the Bi₂Se₃ vdW gap in the contact area injected by voltage pulses.

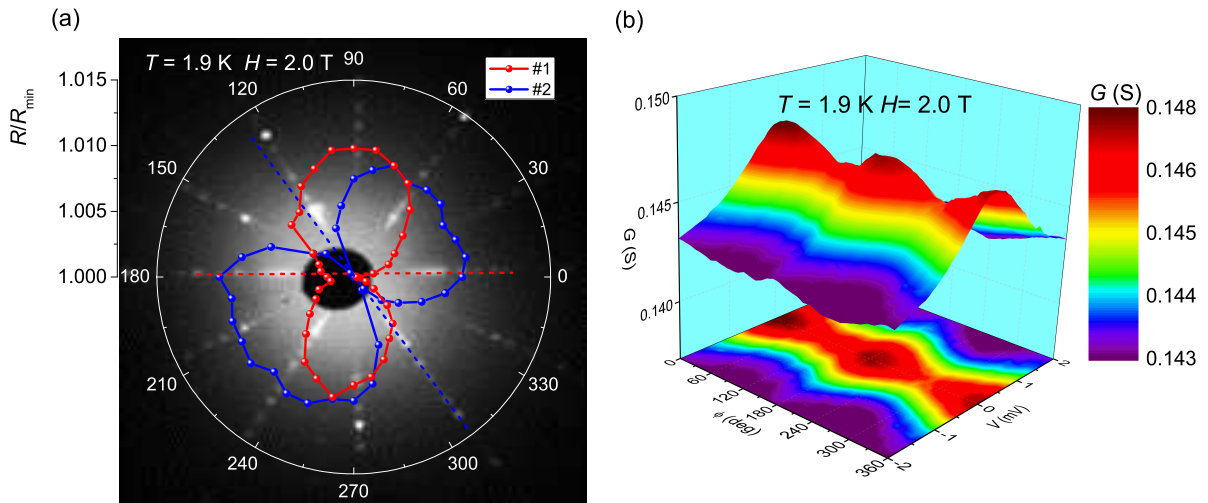


Figure 3: **Field-angle dependence of the soft-PCS of Ag-Bi₂Se₃ with the induced superconductivity.** (a) Field-angle dependence of the ZBR for two contacts #1 and #2 on the same Bi₂Se₃ crystal at 1.9 K with an in-plane field of 2.0 T. The red (blue) dashed line marks the short C_2 axis for its nematic domain #1 (#2), respectively. (b) Three-dimensional contour plot of the soft-PCS conductance curves as a function of field angle at 1.9 K and 2.0 T.

The erasable SC in mesoscopic point-contacts on Bi₂Se₃ with thermal cycles implies a promising application on logic and memory circuits as an electrical switch, if equipped with a local heater on the contact [29, 30, 31, 32]. A voltage pulse can momentarily drive the sample into superconducting state as a low-resistance phase, while an electrical heater can switch it back to the normal state as a high-resistance phase. This can serve as a phase-change memory while its different resistance states represent 1s and 0s for the stored digital data. The local and erasable superconductivity induced with Ag tip signifies a more accurate and controllable writing/design of superconducting circuits (even topological superconducting circuits) at low temperatures, if scanning probe microscopic lithography method can be introduced [22, 33]. We notice a recent work carried out by the conductive-AFM method on two-dimensional electron gas and our results would facilitate such efforts [34, 35].

Finally, we would like to investigate the superconducting nature of the Ag-doped topological insulator Bi₂Se₃ in our mesoscopic point-contacts, where our field-rotational PCS characterizes a rotational C_4 symmetry breaking and suggests an exotic topological SC as in Cu_xBi₂Se₃ [36, 37, 38, 39, 40, 41, 42]. The azimuthal field-angle dependence of the zero-bias point-contact resistance (ZBR) on Bi₂Se₃ after voltage pulse at 1.9 K and in field of 2.0 T is shown in Fig. 3a, where the magnetic field is rotated in the ab -plane. A clear 2-fold symmetry of the ZBR is present at 2.0 T, probably signaling a C_2 symmetry of the superconductor gap and thus a nematic SC despite of its hexagonal lattice structure. This 2-fold symmetry is only observed in the superconducting state below its upper critical field $H_{c2} \sim 3.0$ T but absent in the normal

state as shown in Fig. S2(a). When fixing the field at 2.0 T, the nematic behaviour disappears exactly around its local T_c as in Fig. S2(b) and Fig. S2(c). In our PCS configuration, the junction current is always along the c -axis and perpendicular to the rotational field, so that the influence of vortex motion and Lorentz effect can be excluded. In Fig. 3a, the azimuthal field-angle dependence of ZBR for two different point-contacts #1 and #2 on the same sample both shows an obvious dumbbell shape but with different long C_2 axis, which are perpendicular to the crystal axis and imply the existence of nematic SC domains in Bi_2Se_3 below T_c . It is a strong evidence to exclude other artificial effects as the two-fold origins, such as sample misalignment, sample geometry or point-contact geometry. The existence of different nematic domains is probably caused by the local strain effect and its microscopic mechanism needs further careful studies.

Field-angle dependence of PCS conductance curves at 1.9 K and 2.0 T is shown in Fig. 3b as a three-dimensional contour plot, where a clear 2-fold symmetry can also be observed from both the peak intensity and width of Andreev reflection signals. The anisotropic magnitude of the nematic behaviour can be roughly estimated by the ratio of maximum/minimum conductance peak width with $1.5/1 \sim 1.5$, which is the result of anisotropic upper critical field H_{c2} in the ab -plane. In the Ginzburg-Landau theory, the H_{c2} is inversely proportional to the square-root product of coherence length ξ in two separate directions orthogonal to the field. We can infer that the maximum of coherence length as well as the SC gap minimum in the ab -plane should be along the crystal axis. Such superconductivity is consistent with a fully gapped Δ_{4y} state in an odd-parity E_u symmetry, implying a topological superconductor in the D_{3d} crystal point group [36, 42]. A similar ZBCP in the PCS on $\text{Cu}_x\text{Bi}_2\text{Se}_3$ has been claimed due to Majorana fermions [36, 16], however, we note it can also arise from thermal effect for point-contacts in thermal regimes [17, 43]. Further studies are required to explore the nature and origin of ZBCP for the induced SC in our Ag- Bi_2Se_3 point-contacts.

In conclusion, we have discovered the unexpected superconductivity only in the Ag- Bi_2Se_3 mesoscopic point-contacts by applying a voltage pulse, either in soft- or mechanical- PCS setup, which is rather absent in the case of Au, Cu or Ti contacts within the voltage limit. We propose that the voltage pulse and thus electrical field should inject Ag atoms into the vdW gap of Bi_2Se_3 and induce a local superconductivity. The superconductivity can be erased by thermal cycles, where warming samples up to high temperatures seems to lose the trapped Ag atoms from the weak vdW gap. Our discovery of the erasable and repetitive superconductivity in topological insulator Bi_2Se_3 may pave a new route for applications of quantum electronic devices that harness the power of topological superconductivity and Majorana fermions.

Materials

The high quality Bi_2Se_3 single crystals were offered by Prmat (Shanghai) Technology Co.,

Ltd..

Resistivity measurement

Electrical resistivity of Bi_2Se_3 was measured by the conventional four-probe method. Electrodes on bulk sample of a larger size were made with silver paint (SPI05001-AB), which can be dry within several minutes, while those on the exfoliated Bi_2Se_3 flake were made with pre-sputtered Ag electrodes on Si/SiO₂ chip and the Bi_2Se_3 flake was mechanically transferred on the top of Ag electrodes.

Point-contact spectroscopy measurements

Soft point-contacts on Bi_2Se_3 were prepared by attaching a 20 μm diam. gold wire with a silver-paint drop at the end on the freshly-cleaved surface at room temperature. In such a configuration, thousands of parallel nanoscale channels were assumed between individual silver particles and the crystal surface. Mechanical point-contacts on Bi_2Se_3 in a needle-anvil style were prepared by engaging a sharp tip on the sample surface by piezo-controlled nano-positioners. The tips can be Ag, Au, Cu and Ti wires, with sharp apex cut by razor blade. The conductance curves as a function of bias voltage, $G(V)$, were recorded with the conventional lock-in technique in a quasi-four-probe configuration. The output current is mixed with dc and ac components, which were supplied by the model 6221 Keithley current source and model 7265 DSP lock-in amplifier, respectively. The first harmonic response of the lock-in amplifier is proportional to its point-contact resistance dV/dI as a function of the biased-voltage V .

Low temperature measurements

Resistivity and point-contact spectroscopy down to 1.9 K were measured in a Quantum Design Physical Property Measurement System (14T-PPMS) equipped with a sample rotator.

Pulse application

The voltage pulse is applied by signal generator(Rigol DG 1022) with pulse waveform.

Acknowledgements

We are grateful for valuable discussions with Z.A. Xu, H.Q. Yuan, C. Cao and Y. Liu. This work has been supported by the National Key Research & Development Program of China (Grant No. 2016YFA0300402, No. 2017YFA0303101 and No. 2018YFC0810200) and the National Natural Science Foundation of China (Grant No. 11674279, No. 11374257 and No. 21703204). X.L. would like to acknowledge support from the Zhejiang Provincial Natural Science Foundation of China (LR18A04001). X.W. would like to acknowledge support from Key Research and Development Project of Zhejiang (No. 2018C01048), Zhejiang Lab (No.2018EB0ZX01). We also thank Prmat (Shanghai) Technology Co., Ltd. for their offered Bi_2Se_3 single crystals.

References

- [1] Y. S. Hor, A. J. Williams, J. G. Checkelsky, P. Roushan, J. Seo, Q. Xu, H. W. Zandbergen, A. Yazdani, N. P. Ong, R. J. Cava, [Superconductivity in \$\text{Cu}_x\text{Bi}_2\text{Se}_3\$ and its implications for pairing in the undoped topological insulator](#), Phys. Rev. Lett. 104 (2010) 057001.
- [2] M. X. Wang, C. Liu, J. P. Xu, F. Yang, L. Miao, M. Y. Yao, C. L. Gao, C. Shen, X. Ma, X. Chen, et al., [The coexistence of superconductivity and topological order in the \$\text{Bi}_2\text{Se}_3\$ thin films](#), Science 336 (6077) (2012) 52–55.
- [3] M. Veldhorst, M. Snelder, M. Hoek, T. Gang, V. K. Guduru, X. L. Wang, U. Zeitler, W. G. van der Wiel, A. A. Golubov, H. Hilgenkamp, et al., [Josephson supercurrent through a topological insulator surface state](#), Nature Mater. 11 (5) (2012) 417.
- [4] E. Wang, H. Ding, A. V. Fedorov, W. Yao, Z. Li, Y.-F. Lv, K. Zhao, L.-G. Zhang, Z. Xu, J. Schneeloch, et al., [Fully gapped topological surface states in \$\text{Bi}_2\text{Se}_3\$ films induced by a d-wave high-temperature superconductor](#), Nature Phys. 9 (10) (2013) 621.
- [5] K. Kirshenbaum, P. S. Syers, A. P. Hope, N. P. Butch, J. R. Jeffries, S. T. Weir, J. J. Hamlin, M. B. Maple, Y. K. Vohra, J. Paglione, [Pressure-induced unconventional superconducting phase in the topological insulator \$\text{Bi}_2\text{Se}_3\$](#) , Phys. Rev. Lett. 111 (2013) 087001.
- [6] L. Aggarwal, A. Gaurav, G. S. Thakur, Z. Haque, A. K. Ganguli, G. Sheet, [Unconventional superconductivity at mesoscopic point contacts on the 3D Dirac semimetal \$\text{Cd}_3\text{As}_2\$](#) , Nature Mater. 15 (1) (2016) 32.
- [7] H. Wang, H. Wang, H. Liu, H. Lu, W. Yang, S. Jia, X.-J. Liu, X. Xie, J. Wei, J. Wang, [Observation of superconductivity induced by a point contact on 3D Dirac semimetal \$\text{Cd}_3\text{As}_2\$ crystals](#), Nature Mater. 15 (1) (2016) 38.
- [8] C. Nayak, S. H. Simon, A. Stern, M. Freedman, S. Das Sarma, [Non-Abelian anyons and topological quantum computation](#), Rev. Mod. Phys. 80 (2008) 1083–1159.
- [9] J. Alicea, Y. Oreg, G. Refael, F. Von Oppen, M. P. Fisher, [Non-Abelian statistics and topological quantum information processing in 1D wire networks](#), Nature Phys. 7 (5) (2011) 412.

- [10] R. M. Lutchyn, J. D. Sau, S. Das Sarma, [Majorana fermions and a topological phase transition in semiconductors](#), Phys. Rev. Lett. 105 (2010) 077001.
- [11] A. K. Geim, I. V. Grigorieva, [Van der Waals heterostructures](#), Nature 499 (7459) (2013) 419.
- [12] Y. Liu, Y. Huang, X. Duan, [Van der Waals integration before and beyond two-dimensional materials](#), Nature 567 (7748) (2019) 323.
- [13] D. Basov, M. Fogler, F. G. De Abajo, [Polaritons in van der Waals materials](#), Science 354 (6309) (2016) aag1992.
- [14] N. P. Butch, K. Kirshenbaum, P. Syers, A. B. Sushkov, G. S. Jenkins, H. D. Drew, J. Paglione, [Strong surface scattering in ultrahigh-mobility \$\text{Bi}_2\text{Se}_3\$ topological insulator crystals](#), Phys. Rev. B 81 (2010) 241301.
- [15] D. Kim, Q. Li, P. Syers, N. P. Butch, J. Paglione, S. D. Sarma, M. S. Fuhrer, [Intrinsic electron-phonon resistivity of \$\text{Bi}_2\text{Se}_3\$ in the topological regime](#), Phys. Rev. Lett. 109 (2012) 166801.
- [16] S. Sasaki, M. Kriener, K. Segawa, K. Yada, Y. Tanaka, M. Sato, Y. Ando, [Topological superconductivity in \$\text{Cu}_x\text{Bi}_2\text{Se}_3\$](#) , Phys. Rev. Lett. 107 (2011) 217001.
- [17] G. Sheet, S. Mukhopadhyay, P. Raychaudhuri, [Role of critical current on the point-contact Andreev reflection](#), Phys. Rev. B 69 (2004) 134507.
- [18] T. T. Tsong, [Effects of an electric field in atomic manipulations](#), Phys. Rev. B 44 (1991) 13703–13710.
- [19] S. Koley, S. Basu, [Superconductivity induced by Ag intercalation in Dirac semimetal \$\text{Bi}_2\text{Se}_3\$](#) , arXiv:1904.03698 (2019).
- [20] H. J. Mamin, P. H. Guethner, D. Rugar, [Atomic emission from a gold scanning-tunneling-microscope tip](#), Phys. Rev. Lett. 65 (1990) 2418–2421.
- [21] H. M. Saavedra, T. J. Mullen, P. Zhang, D. C. Dewey, S. A. Claridge, P. S. Weiss, [Hybrid strategies in nanolithography](#), Rep. Prog. Phys. 73 (3) (2010) 036501.
- [22] R. Garcia, A. W. Knoll, E. Riedo, [Advanced scanning probe lithography](#), Nat. Nano. 9 (8) (2014) 577.
- [23] T. Tsong, [Field ion image formation](#), Surface Science 70 (1) (1978) 211–233.

- [24] S. Katano, M. Hotsuki, Y. Uehara, [Creation and luminescence of a single silver nanoparticle on Si \(111\) in](#) J. Phys. Chem. C 120 (50) (2016) 28575–28582.
- [25] M. Olsen, M. Hummelgård, H. Olin, [Surface modifications by field induced diffusion](#), PLoS One 7 (1) (2012) e30106.
- [26] J. A. Schneeloch, R. D. Zhong, Z. J. Xu, G. D. Gu, J. M. Tranquada, [Dependence of superconductivity in \$\text{Cu}_x\text{Bi}_2\text{Se}_3\$ on quenching conditions](#), Phys. Rev. B 91 (2015) 144506.
- [27] H. Oike, M. Kamitani, Y. Tokura, F. Kagawa, [Kinetic approach to superconductivity hidden behind a com](#) Sci. Adv. 4 (10) (2018) eaau3489.
- [28] M. Yoshida, K. Kudo, M. Nohara, Y. Iwasa, [Metastable superconductivity in two-dimensional \$\text{IrTe}_2\$ crystal](#) Nano lett. 18 (5) (2018) 3113–3117.
- [29] G. Meijer, [Who wins the nonvolatile memory race?](#), Science 319 (5870) (2008) 1625–1626.
- [30] D. B. Strukov, G. S. Snider, D. R. Stewart, R. S. Williams, [The missing memristor found](#), Nature 453 (7191) (2008) 80.
- [31] D.-H. Kwon, K. M. Kim, J. H. Jang, J. M. Jeon, M. H. Lee, G. H. Kim, X.-S. Li, G.-S. Park, B. Lee, S. Han, et al., [Atomic structure of conducting nanofilaments in \$\text{TiO}_2\$ resistive switching memory](#), Nat. Nano. 5 (2) (2010) 148.
- [32] K. Szot, W. Speier, G. Bihlmayer, R. Waser, [Switching the electrical resistance of individual dislocations in](#) Nat. Mater. 5 (4) (2006) 312.
- [33] A. A. Tseng, A. Notargiacomo, T. Chen, [Nanofabrication by scanning probe microscope lithography: A re](#) J. Vac. Sci. Tech. B 23 (3) (2005) 877–894.
- [34] Y.-Y. Pai, H. Lee, J.-W. Lee, A. Annadi, G. Cheng, S. Lu, M. Tomczyk, M. Huang, C.-B. Eom, P. Irvin, J. Levy, [One-dimensional nature of superconductivity at the \$\text{LaAlO}_3/\text{SrTiO}_3\$ interface](#), Phys. Rev. Lett. 120 (2018) 147001.
- [35] C. Cen, S. Thiel, G. Hammerl, C. W. Schneider, K. Andersen, C. Hellberg, J. Mannhart, J. Levy, [Nanoscale control of an interfacial metal–insulator transition at room temperature](#), Nature Mater. 7 (4) (2008) 298–302.

- [36] L. Fu, [Odd-parity topological superconductor with nematic order: Application to \$\text{Cu}_x\text{Bi}_2\text{Se}_3\$](#) , Phys. Rev. B 90 (2014) 100509.
- [37] K. Matano, M. Kriener, K. Segawa, Y. Ando, G. Q. Zheng, [Spin-rotation symmetry breaking in the superconducting state of \$\text{Cu}_x\text{Bi}_2\text{Se}_3\$](#) , Nat. Phys. 12 (2016) 852–854.
- [38] S. Yonezawa, K. Tajiri, S. Nakata, Y. Nagai, Z. Wang, K. Segawa, Y. Ando, Y. Maenos, [Thermodynamic evidence for nematic superconductivity in \$\text{Cu}_x\text{Bi}_2\text{Se}_3\$](#) , Nat. Phys. 13 (2017) 123–126.
- [39] T. Asaba, B. J. Lawson, C. Tinsman, L. Chen, P. Corbae, G. Li, Y. Qiu, Y. S. Hor, L. Fu, L. Li, [Rotational symmetry breaking in a trigonal superconductor nb-doped \$\text{Bi}_2\text{Se}_3\$](#) , Phys. Rev. X 7 (2017) 011009.
- [40] R. Tao, Y.-J. Yan, X. Liu, Z.-W. Wang, Y. Ando, Q.-H. Wang, T. Zhang, D.-L. Feng, [Direct visualization of the nematic superconductivity in \$\text{Cu}_x\text{Bi}_2\text{Se}_3\$](#) , Phys. Rev. X 8 (2018) 041024.
- [41] Y. Sun, S. Kittaka, T. Sakakibara, K. Machida, J. Wang, J. Wen, X. Xing, Z. Shi, T. Tamegai, [Quasiparticle evidence for the nematic state above \$\text{Sr}_x\text{Bi}_2\text{Se}_3\$](#) , Phys. Rev. Lett. 123 (2019) 027002.
- [42] J. W. F. Venderbos, V. Kozii, L. Fu, [Odd-parity superconductors with two-component order parameters: N](#), Phys. Rev. B 94 (2016) 180504.
- [43] D. Dagher, R. S. Gonnelli, [Probing multiband superconductivity by point-contact spectroscopy](#), Supercond. Sci. Technol. 23 (4) (2010) 043001.